

1 **Mechanistic dissection of alga recognition and uptake in coral-algal**
2 **endosymbiosis**
3

4 Minjie Hu*, Yun Bai, Xiaobin Zheng & Yixian Zheng*

5
6 Department of Embryology, Carnegie Institution for Science, Baltimore, MD, USA
7 e-mail: mhu2@carnegiescience.edu; zheng@carnegiescience.edu

8 **Abstract**

9 Many corals form a mutually beneficial relationship with the dinoflagellate
10 algae called *Symbiodiniaceae*. Cells in the coral gastrodermis recognize,
11 phagocytose, and house the algae in an organelle called symbiosome, which
12 supports algae photosynthesis and nutrient exchange with corals^{1–3}. Rising ocean
13 temperature disrupts this endosymbiotic relationship, leading to alga loss, coral
14 bleaching and death, and the degradation of marine ecosystems^{4–6}. Mitigation of
15 coral death requires a mechanistic understanding of coral-algal endosymbiosis.
16 We have developed genomic resources to enable the use of a soft coral *Xenia*
17 species as a model to study coral-algal endosymbiosis⁷. Here we report an effective
18 RNA interference (RNAi) method and its application in the functional studies of
19 genes involved in early steps of endosymbiosis. We show that an endosymbiotic
20 cell marker called LePin (for its Lectin and kazal Protease inhibitor domains) is a
21 secreted lectin that binds to algae to initiate the formation of alga-containing
22 endosymbiotic cells. The evolutionary conservation of LePin among marine
23 endosymbiotic anthozoans suggests a general role in coral-algal recognition.
24 Coupling bioinformatics analyses with RNAi and single cell (sc)-RNA-seq, we
25 uncover three gene expression programs (GEP) influenced by LePin during the
26 early and middle stages of endosymbiotic lineage development. Further studies of
27 genes in these GEPs lead to the identification of two scavenger receptors that
28 support the formation of alga-containing endosymbiotic cells, most likely by
29 initiating phagocytosis and modulating coral immune response. We also identify
30 two actin regulators for endosymbiosis, which shed light on the phagocytic

31 **machinery and a possible mechanism for symbosome formation. Our findings**
32 **should usher in an era of mechanistic studies of coral-algal endosymbiosis.**

33

34 **Main**

35 The importance of endosymbiosis for corals has been recognized for many
36 decades^{8,9}, but the biology of this mutually beneficial relationship remains obscure
37 because it has been subject to limited molecular studies. The alarming loss of coral reefs
38 and the associated degradation of marine environments have galvanized efforts to
39 understand coral-algal endosymbiosis in recent years. Multiple bulk RNA-seq
40 comparisons between apo-endosymbiotic and endosymbiotic corals or control and
41 bleached corals have identified a large number of differentially expressed genes.
42 Although these genes could be candidate regulators for endosymbiosis, many of them,
43 such as the NFkB pathway genes and lectin genes^{10–13}, may be expressed in different
44 cell types and have general functions beyond endosymbiosis. Their differential
45 expression may represent a secondary response to alga loss. Through developing *Xenia*
46 as a model organism for studying coral endosymbiosis, we have identified different cell
47 types based on scRNA-seq and established methods to characterize lineage progression
48 of the endosymbiotic cell type⁷. Among the genes highly expressed in *Xenia*
49 endosymbiotic cells, 89 are markers for the endosymbiotic cell lineage because they are
50 specifically expressed in this cell type, while an additional 686 highly expressed genes in
51 endosymbiotic cells are also found in a few other cell types⁷. Interestingly, some of these
52 genes are conserved and specifically expressed in the endosymbiotic cells of a stony
53 coral as revealed by a recent study¹⁴. Functional analyses of these genes could yield

54 mechanistic insights of coral endosymbiosis. Such insights are important for
55 understanding how corals bleach and it may aid in developing mitigation strategies. For
56 example, recent studies suggest that corals harboring heat resistant algae are more
57 resistant to bleaching than those corals selecting the non-heat resist endosymbionts^{15–18}.
58 Identifying the algal selection mechanism could help engineering heat resistant corals.

59

60 **RNA interference as an efficient means for gene down regulation in *Xenia* sp.**

61 Our genomic study has found key components of RNA interference (RNAi)
62 machinery in *Xenia*⁷. Since corals are known to actively take up fluids from the
63 environment through macropinocytosis¹⁹, simple incubation of *Xenia* with RNAi oligos
64 could result in uptake of the oligos and RNAi-mediated gene silencing. We tested this by
65 incubating *Xenia* polyps with media containing Cy3-labeled oligo-T for a day and found
66 strong Cy3 signals in *Xenia* tissues (Fig. 1a). We next synthesized control short hairpin
67 RNA (shRNA) and shRNAs targeting *Xenia* genes predicted to encode tubulin, GAPDH,
68 and lamin-B2 (Supplementary Table S1), and incubated them with *Xenia* polyps. As
69 shown by Real-Time Quantitative Reverse Transcription PCR (RT-qPCR), the shRNAs
70 substantially reduced the expression of these genes compared to the control (Fig. 1b).
71 Thus, the RNAi approach should allow us to establish the function and dissect the
72 mechanism of candidate genes required for endosymbiosis.

73

74 **LePin aids the formation of new alga-containing endosymbiotic cells**

75 During lineage progression of *Xenia* endosymbiotic cells, the formation of alga-
76 containing cells begins when progenitor cells select and bind to the correct

77 *Symbiodiniaceae* species. Lectins are a family of pattern recognition proteins known to
78 exhibit binding specificity to different glycans on microbial surfaces²⁰. They have been
79 implicated in alga selection/recognition during coral endosymbiosis^{21–23}. Finding the lectin
80 specifically involved in selecting/recognizing the preferred endosymbiotic algae among
81 numerous lectins in a given cnidarian genome²⁴ has been challenging. We previously
82 identified expression of a lectin called LePin as a marker for the *Xenia* endosymbiotic cell
83 type⁷. Using sequence analyses, we found LePin-like proteins with similar domain
84 compositions in the endosymbiotic marine anthozoans, while the most similar lectins in a
85 non-endosymbiotic marine anthozoan, *Nematostella*, lacked the C-lectin and EGF
86 domains (Extended Data Fig. 1). This suggests that LePin could be the lectin involved in
87 initiating endosymbiosis by recognizing proper endosymbiotic algae for corals. To study
88 the role of LePin, we designed two shRNAs targeting different regions of LePin (Extended
89 Data Fig. 2a). *LePin* expression was efficiently reduced by both shRNAs in intact *Xenia*
90 polyps or polyps undergoing regeneration after tentacle amputation⁷ (Fig. 1c). Since
91 *LePin* is strongly and specifically expressed in the endosymbiotic lineage in *Xenia*, its
92 down regulation is specific in cells of this lineage.

93 Next, we performed scRNA-seq using the regenerating *Xenia* polyps treated by
94 control or LePin shRNA (Extended Data Fig. 3). Previously, we established the stages of
95 endosymbiotic lineage progression using trajectory analyses based on scRNA-seq of
96 either full grown *Xenia* polyps or polyps undergoing regeneration after tentacle
97 amputation^{7,25}. Using scRNA-seq, we established gene expression patterns of the
98 endosymbiotic cells as they progress from alga-free progenitors to alga-carrying cells,
99 and finally to cells with gene expression patterns suggesting that they are post

100 endosymbiotic (algae free)⁷. This lineage progression was supported by ethynyl
101 deoxyuridine (EdU) pulse-chase to track the newly divided *Xenia* cells that take up algae⁷.
102 We constructed the trajectory of endosymbiotic cell lineage progression based on the
103 scRNA-seq of the shRNA-treated samples and analyzed the cell distribution along the
104 trajectory (Fig. 2a). We then utilized our previously identified genes enriched in the
105 progenitor endosymbiotic cells⁷ and mapped them in the new trajectory. Most of the genes
106 showed highest expression in the progenitor cells in both control and *LePin* RNAi-treated
107 samples (Fig. 2b, Extended Data Fig. 4), confirming the direction of lineage progression
108 (Fig. 2a). The major peaks in the control and *LePin* shRNA-treated samples represent the
109 alga-containing endosymbiotic cells because their gene expression patterns are highly
110 similar to the transcriptome of the *Xenia* alga-containing cells isolated by Fluorescence
111 Activated Cell Sorting (FACS)⁷. *LePin* RNAi resulted in an increased accumulation of cells
112 prior to the major peak (Fig. 2a, yellow arrow). We then applied the EdU pulse-chase to
113 trace the newly formed endosymbiotic cells in the regenerating *Xenia* treated by control
114 or *LePin* shRNA (Fig. 2c). Using our previously established FACS analysis method⁷, we
115 found a significant reduction in the newly divided cells (EdU+) that contained algae upon
116 *LePin* RNAi (Fig. 2d). Thus, *LePin* supports the formation of new alga-containing
117 endosymbiotic cells.

118

119 **LePin influences three gene expression programs containing candidate genes for**
120 **early and mid-stages of endosymbiotic lineage progression**

121 As a lectin, *LePin* could be involved in initiating alga selection, recognition, and
122 subsequent steps of endosymbiosis. If it served any of these roles, elimination of *LePin*

123 would be expected to impact gene expression programs of the endosymbiotic cells.
124 Applying non-negative matrix factorization (NMF) to scRNA-seq data, it is possible to
125 computationally identify co-expressed genes in individual cells, called metagenes or gene
126 expression programs (GEPs)^{26–28}. GEPs may govern cell type identities and/or cell
127 activities²⁸. Therefore identifying the GEPs with altered expression upon *LePin*
128 knockdown could facilitate the discovery of genes involved in endosymbiosis. We applied
129 NMF to the endosymbiotic cell lineage and identified 24 GEPs (Supplementary Table S2).
130 We then coupled the lineage trajectory with the NMF analysis to uncover the GEP
131 expression levels of the 24 GEPs in individual cells during endosymbiotic lineage
132 development (Fig. 2e). We reasoned that comparisons of the expression of GEPs in
133 control and *LePin* RNAi-treated samples along the lineage progression may allow us to
134 identify the candidate GEPs that regulate endosymbiosis (Supplementary Table S3).
135 Among the GEPs that showed expression changes upon *LePin* RNAi, we found three,
136 GEP1, 4, and 22, that showed changes during the early and middle stages of
137 endosymbiotic cell lineage development (Fig. 2f-h). This suggests that the three GEPs
138 contain genes that function at a relatively early stage of endosymbiosis and are affected
139 by *LePin* function. Since *LePin* is one of the top 30 weighted genes that contribute most
140 to the GEP1 (Supplementary Table S2), we randomly selected two genes in this GEP
141 based on the gene IDs, Xe_016304 and Xe_011936. Xe_016304 is predicted to encode
142 a Heme binding protein (Heme binding protein 2_1), while Xe_011936 is predicted to
143 encode a protein containing two domains, OmpH (Outer membrane protein H) and FReD
144 (Fibrinogen-related domain, FibL) and we referred to this protein as OmpH/FibL⁷
145 (Extended Data Fig. 2b). We previously identified the *OmpH/FibL* gene as one of the 89

146 endosymbiotic cell markers, while Heme binding protein 2_1 (*Heme-binding2*) is one of
147 the 686 highly expressed genes in the endosymbiotic cells⁷. RNAi of each of the two
148 genes resulted in a significant reduction of newly formed alga-containing endosymbiotic
149 cells (Fig. 2i). Thus, the three GEPs contain promising candidates to be involved in
150 mediating early steps of endosymbiosis.

151

152 **LePin binds to algae and mediates their interaction with *Xenia* gastrodermis**

153 To further understand the role of LePin in alga recognition, we analyzed *Xenia*
154 tissue sections cut across tentacles, the region connecting tentacles to the mouth
155 (tentacle_mouth), the region connecting the stalk to the mouth (stalk_mouth), and stalks
156 (see the illustrations in the inserts in Fig. 3a). As indicated by nuclear staining, the mouth
157 tissue has an opening in the center surrounded by densely packed cells compared to all
158 the other regions in the polyp (Fig. 3a, M, mouth outlined by white dotted lines). We found
159 numerous algae at or near the gastrodermis surfaces of these regions (Fig. 3a). We next
160 developed an unbiased and high throughput method (Extended Data Fig. 5 and Method)
161 to quantify the number of algae at the surface of gastrodermis throughout the tissue
162 sections from the regenerating *Xenia* treated by control or *LePin* shRNA. We found that
163 the *Xenia* stalk_mouth region showed a significant reduction of algae attachment upon
164 *LePin* RNAi (Fig. 3b). Thus, LePin may initiate algae uptake by supporting the interaction
165 between algae and the gastrodermis cells in the stalk-mouth region.

166 To further understand how LePin mediates alga recognition, we analyzed the
167 LePin sequence and uncovered a signal peptide at its N-terminus²⁹, but we found no
168 transmembrane domains³⁰ (Extended Data Fig. 6). This suggests that LePin is a secreted

169 lectin. We next produced antibodies to peptides corresponding to two regions of LePin
170 (Extended Data Fig. 2) and affinity purified the antibodies using the peptides. We
171 performed LePin antibody staining of *Xenia* tissue sections and found LePin on the
172 surface of the mouth tissues (Fig. 4a). RNAi of LePin resulted in a significant reduction of
173 these LePin signals (Fig. 4a top right panels and 4b), demonstrating that LePin is present
174 on the surface of mouth tissue. This is consistent with LePin being a secreted lectin. Since
175 the mouth region of a scleractinian coral, *fungia scutaria*, has been implicated in
176 mediating endosymbiosis establishment in the larvae³¹, the LePin on the *Xenia* mouth
177 surface could aid the recognition/selection of algae as they enter into the gastrodermis.

178 To understand how LePin could help alga recognition/selection, we treated the
179 regenerating *Xenia* polyps with control or *LePin* shRNA and then isolated the free algae
180 from these animals. Immunostaining using control and LePin antibodies revealed various
181 levels of LePin signals on the surface of these algae (Fig. 4c). We performed FACS-
182 based unbiased quantification of the LePin signal on algae. Since the algae
183 autofluorescence precluded detection of weak LePin signals on algae, we focused on
184 algae with strong LePin signals. We found that *LePin* shRNA significantly reduced the
185 percentage of algae with strong LePin signals (Fig. 4d, Extended Data Fig. 7). Therefore
186 the secreted LePin can recognize and bind free algae.

187 Since LePin RNAi caused a significant reduction of algae attached to the
188 gastrodermis of the stalk-mouth region, we next focused on the analysis of LePin in this
189 region. Although a large number of algae in this region made it difficult to detect LePin
190 signal due to a high background signal of algal autofluorescence, we were able to detect
191 clear LePin signals in some cells that do not appear to contain algae and the signal was

192 significantly diminished by *LePin* shRNA (Fig. 4a, bottom panels and 4e). Together, these
193 findings support a role of *LePin* in mediating the binding of algae to the progenitor
194 endosymbiotic cells to aid the interaction with algae in the stalk-mouth region of the
195 gastrodermis.

196

197 **Identification of scavenger receptors and actin regulators for endosymbiosis**

198 Upon binding to the endosymbiotic algae, coral cells must activate the phagocytic
199 pathway for alga uptake. As a secreted protein, *LePin* needs to use phagocytic
200 receptors to initiate phagocytosis. We examined genes in the GEP1, 4, and 22 and
201 found a number of genes predicted to encode scavenger receptors (Supplementary
202 Table S2). The scavenger receptors are known to recognize common ligands on
203 microbial surfaces and are implicated in initiating microbial phagocytosis^{32,33}. We
204 performed shRNA treatment and found that shRNA targeting of each of two scavenger
205 receptor genes, *CD36* and *DMBT1*, resulted in a significant reduction of the newly
206 formed alga-containing endosymbiotic cells (Fig. 5a, Extended Data Fig. 2c). Both
207 *CD36* and *DMBT1* were previously identified as marker genes for the *Xenia*
208 endosymbiotic cell type⁷. Additionally, sequence analyses showed that the *Xenia* *CD36*
209 has an N- and C-terminal transmembrane domains similar to the *CD36* known to initiate
210 microbe phagocytosis and host immune response in the well-established model
211 organisms^{34,35}. *DMBT1* has an established role in modulating immune response in the
212 mucosal surfaces in mammals^{36,37}. Thus, these two scavenger receptors may function
213 downstream of *LePin* to engage the phagocytic machinery and modulate *Xenia*
214 immunity for algae uptake.

215 To establish endosymbiosis, *Xenia* needs to not only phagocytose the
216 endosymbiotic algae, but also repress the fusion of the alga-containing phagosomes
217 with lysosomes, thereby supporting the conversion of phagosomes to symbiosomes³⁸.
218 Actomyosin assembly is required for phagocytic target search and capture, formation of
219 phagocytic cup, the subsequent phagosome formation and maturation³⁹. Additionally,
220 the disassembly of actin cables on the phagosome surfaces can aid phagosome
221 maturation through fusion with endosomes and lysosome⁴⁰. By surveying the GEP1, 4,
222 and 22, we found two genes encoding conserved actin regulators, PLEKHG5 and
223 SWAP70, in GEP4 and 22 (Supplementary Table S2, Extended Data Fig. 2d).
224 PLEKHG5 is a marker for endosymbiotic cells and as a RhoGTPase guanine nucleotide
225 exchange factor (RhoGEF), PLEKHG5 can regulate actomyosin assembly at the
226 plasma membrane⁴¹. SWAP70 stimulates actin cable formation on phagosome
227 membranes during phagocytosis and may inhibit phagosome maturation and fusion with
228 lysosomes⁴². We found that RNAi of either gene resulted in a significant reduction of
229 newly formed alga-containing endosymbiotic cells (Fig. 5b). This suggests that the two
230 proteins are part of the phagocytic machinery functioning downstream of scavenger
231 receptors to enable algae phagocytosis. By favoring actin cable assembly on the
232 phagosome surface⁴², SWAP70 could delay phagolysosome fusion and aid
233 symbiosome formation in *Xenia*.

234

235 **Summary and outlook**

236 Through developing an efficient RNAi protocol, we have identified a secreted
237 lectin, LePin, that supports the formation of alga-containing endosymbiotic cells in

238 *Xenia*. Since LePin interacts with algae and appears to facilitate their binding to the
239 stalk and mouth region of *Xenia* gastrodermis, it may function in the selection of specific
240 *Symbiodiniaceae* species for *Xenia* endosymbiosis. It is known that corals use a select
241 set of *Symbiodiniaceae* species for endosymbiosis and the corals that select the heat
242 resistant *Symbiodiniaceae* exhibit resistance to heat-induced bleaching^{15,43}. Since
243 lectins can recognize specific glycans found on algal surface, further comparative
244 studies of LePin-like lectins in various corals and their cognate *Symbiodiniaceae* may
245 lead to identification of the LePin sequence motif that selects for heat resistant algae.
246 With the availability of CRISPR (Clustered Regularly Interspaced Short Palindromic
247 Repeats) for coral gene editing⁴⁴, it could then be possible to engineer heat sensitive
248 corals by editing LePin to allow their selection for heat resistant algae. This could offer a
249 possible biological mitigation for coral reefs in the face of global warming.

250 We also demonstrate the power of applying bioinformatics tools to identify gene
251 expression programs that contain important regulators of endosymbiosis. These genes
252 could serve as a great resource for the field for discovery of additional regulators of
253 endosymbiosis. By focusing on the GEPs whose expressions are influenced by LePin
254 during early and mid-stages of endosymbiosis, we identified genes that function during
255 early steps of alga uptake (Fig. 5c). With two transmembrane domains, the *Xenia* CD36
256 we report here is likely to trigger phagocytosis of the LePin bound algae attached to the
257 newly divided endosymbiotic cells. CD36 may also regulate *Xenia* immune response via
258 its N and C-terminal cytoplasmic sequences because the CD36 in the well-established
259 model organisms is known to engage various innate immune pathways upon microbe
260 binding and phagocytosis. *Xenia* and mammalian DMBT1 are highly similar in their

261 multiple scavenger receptor domains. Mammalian DMBT1 can suppress inflammation³⁶.
262 Further study of these *Xenia* scavenger receptors could provide mechanistic insights on
263 algae uptake and immune modulation critical for endosymbiosis. The *Xenia* PLEKHG5
264 and SWAP70 are conserved actin regulators that can mediate phagocytosing algae and
265 phagosome formation. Since symbiosomes are derived from phagosomes and since
266 SWAP70 is implicated in delaying phagosome maturation in mammalian cells, further
267 study of the *Xenia* SWAP70 could facilitate the understanding of how symbiosomes are
268 derived from phagosomes to aid nutrients exchange between coral and algae.

269

270 **References**

- 271 1. Davy, S. K., Allemand, D. & Weis, V. M. Cell biology of cnidarian-dinoflagellate
272 symbiosis. *Microbiol Mol Biol Rev* **76**, 229–61 (2012).
- 273 2. Tang, B. L. Thoughts on a very acidic symbiosome. *Front. Microbiol.* **6**, (2015).
- 274 3. Barott, K. L., Venn, A. A., Perez, S. O., Tambutté, S. & Tresguerres, M. Coral host cells
275 acidify symbiotic algal microenvironment to promote photosynthesis. *Proc. Natl. Acad. Sci.*
276 **112**, 607–612 (2015).
- 277 4. Hughes, T. P. *et al.* Climate Change, Human Impacts, and the Resilience of Coral Reefs.
278 *Science* **301**, 929–933 (2003).
- 279 5. Hughes, T. P. *et al.* Global warming and recurrent mass bleaching of corals. *Nature* **543**,
280 373–377 (2017).
- 281 6. Rädecker, N. *et al.* Heat stress destabilizes symbiotic nutrient cycling in corals. *Proc. Natl.*
282 *Acad. Sci.* **118**, e2022653118 (2021).
- 283 7. Hu, M., Zheng, X., Fan, C.-M. & Zheng, Y. Lineage dynamics of the endosymbiotic cell

284 type in the soft coral *Xenia*. *Nature* **582**, 534–538 (2020).

285 8. Roth, M. S. The engine of the reef: photobiology of the coral–algal symbiosis. *Front.*
286 *Microbiol.* **5**, (2014).

287 9. Jinkerson, R. E. *et al.* Cnidarian-Symbiodiniaceae symbiosis establishment is independent of
288 photosynthesis. *Curr. Biol.* **32**, 2402-2415.e4 (2022).

289 10. Pinzón, J. H. *et al.* Whole transcriptome analysis reveals changes in expression of immune-
290 related genes during and after bleaching in a reef-building coral. *R. Soc. Open Sci.* **2**, 140214
291 (2015).

292 11. Mohamed, A. R. *et al.* The transcriptomic response of the coral *Acropora digitifera* to a
293 competent *Symbiodinium* strain: the symbiosome as an arrested early phagosome. *Mol Ecol*
294 **25**, 3127–41 (2016).

295 12. Mohamed, A. R. *et al.* Dual RNA-sequencing analyses of a coral and its native symbiont
296 during the establishment of symbiosis. *Mol. Ecol.* **29**, 3921–3937 (2020).

297 13. Yoshioka, Y., Yamashita, H., Suzuki, G. & Shinzato, C. Larval transcriptomic responses of a
298 stony coral, *Acropora tenuis*, during initial contact with the native symbiont, *Symbiodinium*
299 *microadriaticum*. *Sci Rep* **12**, 2854 (2022).

300 14. Levy, S. *et al.* A stony coral cell atlas illuminates the molecular and cellular basis of coral
301 symbiosis, calcification, and immunity. *Cell* **184**, 2973-2987 e18 (2021).

302 15. Berkelmans, R. & van Oppen, M. J. H. The role of zooxanthellae in the thermal tolerance of
303 corals: a ‘nugget of hope’ for coral reefs in an era of climate change. *Proc. R. Soc. B Biol.*
304 *Sci.* **273**, 2305–2312 (2006).

305 16. Logan, C. A., Dunne, J. P., Ryan, J. S., Baskett, M. L. & Donner, S. D. Quantifying global
306 potential for coral evolutionary response to climate change. *Nat. Clim. Change* **11**, 537–542

307 (2021).

308 17. Caruso, C., Hughes, K. & Drury, C. Selecting Heat-Tolerant Corals for Proactive Reef
309 Restoration. *Front. Mar. Sci.* **8**, (2021).

310 18. Buerger, P. *et al.* Heat-evolved microalgal symbionts increase coral bleaching tolerance. *Sci.*
311 *Adv.* **6**, eaba2498 (2020).

312 19. Ganot, P. *et al.* Ubiquitous macropinocytosis in anthozoans. *Elife* **9**, (2020).

313 20. Mattox, D. E. & Bailey-Kellogg, C. Comprehensive analysis of lectin-glycan interactions
314 reveals determinants of lectin specificity. *PLOS Comput. Biol.* **17**, e1009470 (2021).

315 21. Koike, K. *et al.* Octocoral chemical signaling selects and controls dinoflagellate symbionts.
316 *Biol Bull* **207**, 80–6 (2004).

317 22. Wood-Charlson, E. M., Hollingsworth, L. L., Krupp, D. A. & Weis, V. M. Lectin/glycan
318 interactions play a role in recognition in a coral/dinoflagellate symbiosis. *Cell Microbiol* **8**,
319 1985–93 (2006).

320 23. Kita, A., Jimbo, M., Sakai, R., Morimoto, Y. & Miki, K. Crystal structure of a symbiosis-
321 related lectin from octocoral. *Glycobiology* **25**, 1016–1023 (2015).

322 24. Wood-Charlson, E. M. & Weis, V. M. The diversity of C-type lectins in the genome of a
323 basal metazoan, *Nematostella vectensis*. *Dev Comp Immunol* **33**, 881–9 (2009).

324 25. Saelens, W., Cannoodt, R., Todorov, H. & Saeys, Y. A comparison of single-cell trajectory
325 inference methods. *Nat Biotechnol* **37**, 547–554 (2019).

326 26. Lee, D. D. & Seung, H. S. Learning the parts of objects by non-negative matrix factorization.
327 *Nature* **401**, 788–91 (1999).

328 27. Siebert, S. *et al.* Stem cell differentiation trajectories in *Hydra* resolved at single-cell
329 resolution. *Science* **365**, eaav9314 (2019).

330 28. Kotliar, D. *et al.* Identifying gene expression programs of cell-type identity and cellular
331 activity with single-cell RNA-Seq. *eLife* **8**, e43803 (2019).

332 29. Almagro Armenteros, J. J. *et al.* SignalP 5.0 improves signal peptide predictions using deep
333 neural networks. *Nat. Biotechnol.* **37**, 420–423 (2019).

334 30. Krogh, A., Larsson, B., von Heijne, G. & Sonnhammer, E. L. Predicting transmembrane
335 protein topology with a hidden Markov model: application to complete genomes. *J. Mol.*
336 *Biol.* **305**, 567–580 (2001).

337 31. Schwarz, J. A., Krupp, D. A. & Weis, V. M. Late Larval Development and Onset of
338 Symbiosis in the Scleractinian Coral *Fungia scutaria*. *Biol Bull* **196**, 70–9 (1999).

339 32. Taban, Q., Mumtaz, P. T., Masoodi, K. Z., Haq, E. & Ahmad, S. M. Scavenger receptors in
340 host defense: from functional aspects to mode of action. *Cell Commun Signal* **20**, 2 (2022).

341 33. Neubauer, E. F., Poole, A. Z., Weis, V. M. & Davy, S. K. The scavenger receptor repertoire
342 in six cnidarian species and its putative role in cnidarian-dinoflagellate symbiosis. *PeerJ* **4**,
343 e2692 (2016).

344 34. Silverstein, R. L. & Febbraio, M. CD36, a scavenger receptor involved in immunity,
345 metabolism, angiogenesis, and behavior. *Sci. Signal.* **2**, re3 (2009).

346 35. Stuart, L. M. *et al.* Response to *Staphylococcus aureus* requires CD36-mediated
347 phagocytosis triggered by the COOH-terminal cytoplasmic domain. *J. Cell Biol.* **170**, 477–
348 485 (2005).

349 36. Reichhardt, M. P., Holmskov, U. & Meri, S. SALSA—A dance on a slippery floor with
350 changing partners. *Mol. Immunol.* **89**, 100–110 (2017).

351 37. Rosenstiel, P. *et al.* Regulation of DMBT1 via NOD2 and TLR4 in Intestinal Epithelial Cells
352 Modulates Bacterial Recognition and Invasion. *J. Immunol.* **178**, 8203–8211 (2007).

353 38. Fransolet, D., Roberty, S. & Plumier, J.-C. Establishment of endosymbiosis: The case of
354 cnidarians and Symbiodinium. *J. Exp. Mar. Biol. Ecol.* **420–421**, 1–7 (2012).

355 39. Vorselen, D. *et al.* Phagocytic ‘teeth’ and myosin-II ‘jaw’ power target constriction during
356 phagocytosis. *eLife* **10**, e68627 (2021).

357 40. Liebl, D. & Griffiths, G. Transient assembly of F-actin by phagosomes delays phagosome
358 fusion with lysosomes in cargo-overloaded macrophages. *J. Cell Sci.* **122**, 2935–2945
359 (2009).

360 41. Popov, I. K., Ray, H. J., Skoglund, P., Keller, R. & Chang, C. The RhoGEF protein Plekhg5
361 regulates apical constriction of bottle cells during gastrulation. *Development* **145**, dev168922
362 (2018).

363 42. Baranov, M. V. *et al.* SWAP70 Organizes the Actin Cytoskeleton and Is Essential for
364 Phagocytosis. *Cell Rep.* **17**, 1518–1531 (2016).

365 43. Silverstein, R. N., Correa, A. M. & Baker, A. C. Specificity is rarely absolute in coral-algal
366 symbiosis: implications for coral response to climate change. *Proc Biol Sci* **279**, 2609–18
367 (2012).

368 44. Cleves, P. A., Strader, M. E., Bay, L. K., Pringle, J. R. & Matz, M. V. CRISPR/Cas9-
369 mediated genome editing in a reef-building coral. *Proc Natl Acad Sci U A* **115**, 5235–5240
370 (2018).

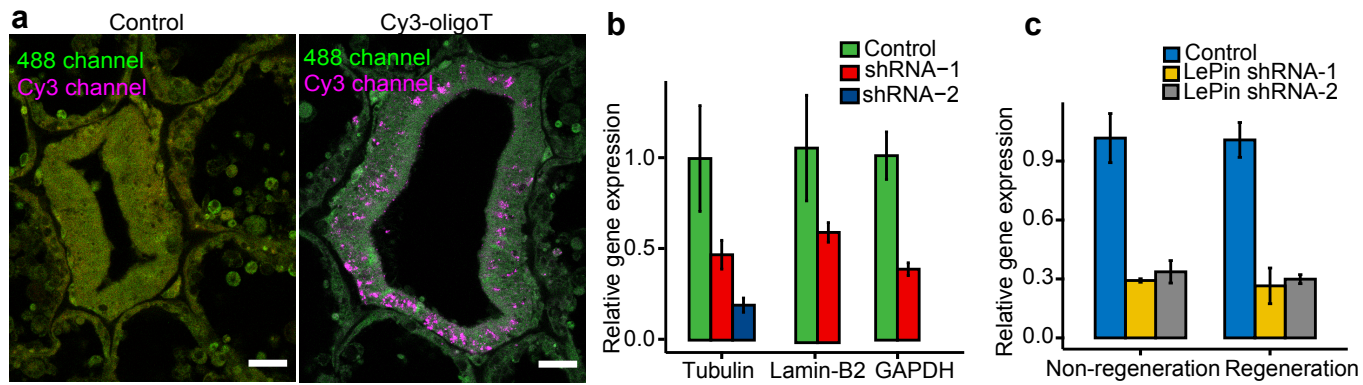


Fig. 1. shRNA knockdown of genes in *Xenia*. **a**, Incubation of *Xenia* polyps in artificial sea water containing Cy3-labeled oligoT (20 nucleotides in length, displayed in magenta) resulted in an uptake of the labeled oligos into tissues. The background signal in the 488 channel (displayed in green) was used to help visualize the outline of tissue sections. Scale bar, 20 μ m. **b,c**, shRNA-mediated knockdown of genes predicted to encode for tubulin, lamin-B2, GAPDH (**b**), and LePin (**c**). For LePin, shRNA is effective for both unperturbed polyps and tentacle amputated polyps undergoing regeneration. Gene expressions are quantified by qRT-PCR. The number of shRNA used for each gene is indicated. Three different polyps were used for each shRNA treatment.

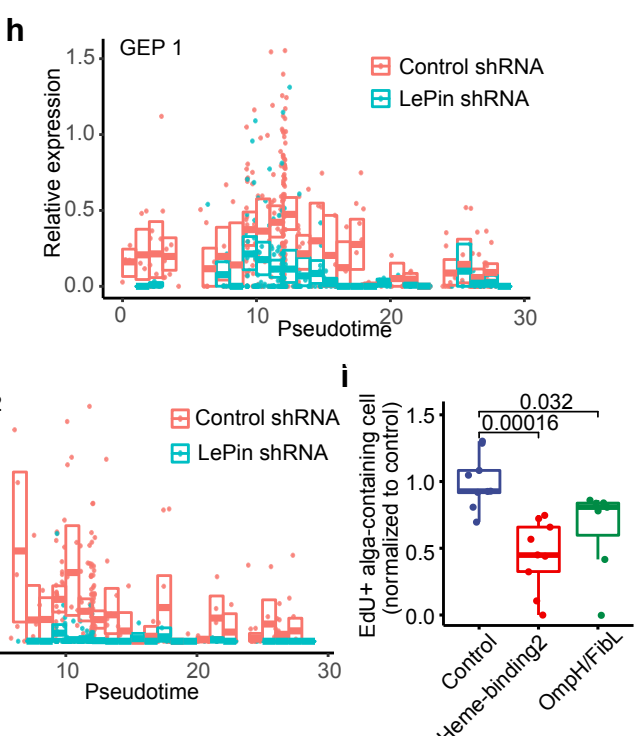
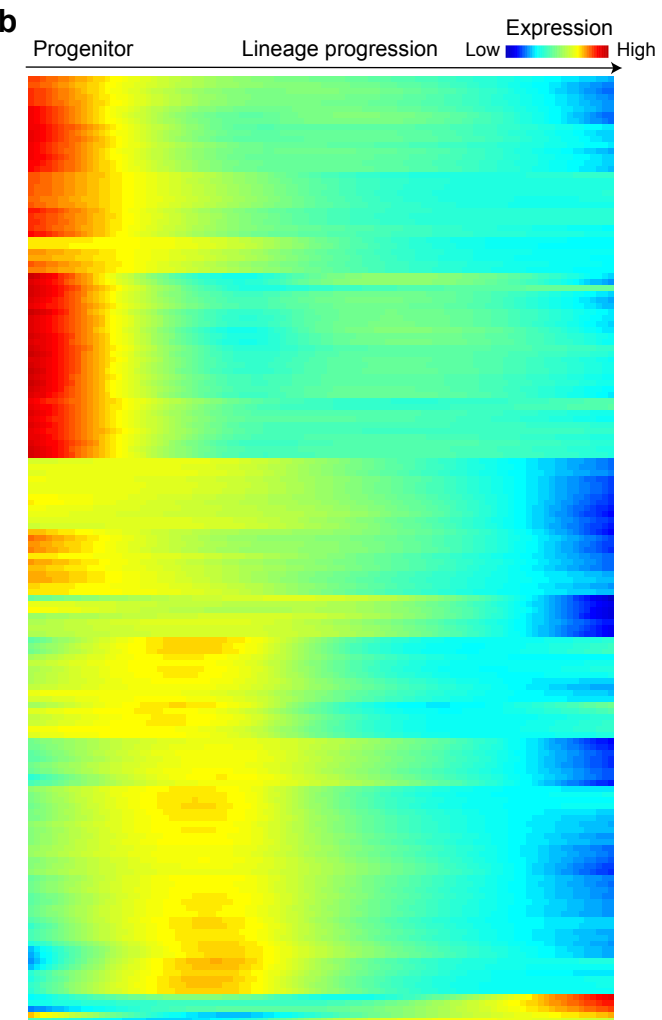
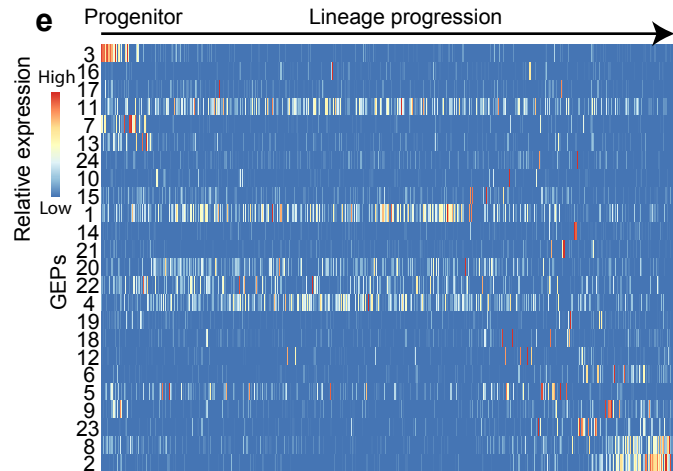
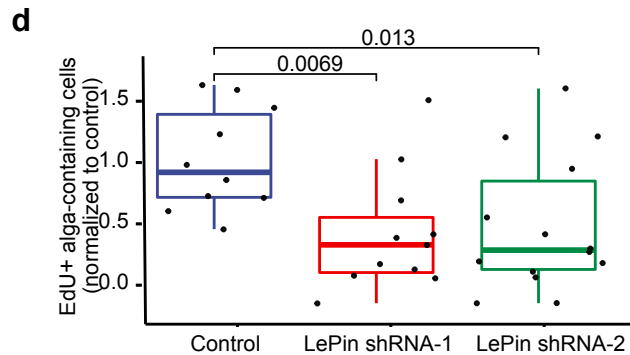
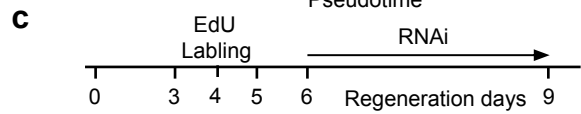
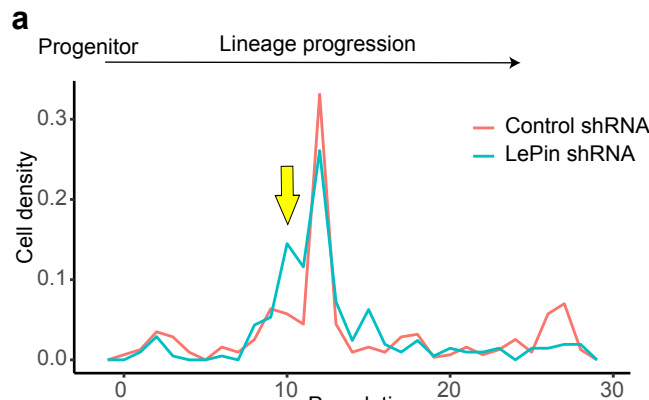
Fig. 2

Fig. 2. LePin aids the formation of new alga-containing cells and impacts gene expression in the endosymbiotic cell lineage. **a**, Endosymbiotic cell distribution along the lineage developmental trajectories based on the scRNA-seq of control and LePin shRNA-treated regenerating polyps. The pseudotime is calculated by Monocle and used to display the lineage trajectory. Yellow arrow indicates a population of cells accumulated prior to the major peak upon LePin RNAi. **b**, Heat map of gene expression along the developmental progression as measured by scRNA-seq. Most previously defined genes expressed in the progenitor endosymbiotic cells (not carrying algae) have higher expression during the early stages of lineage progress than later stages in the new trajectory analysis. **c**, Experimental design for tracking the newly formed alga-containing endosymbiotic cells. EdU was used to label newly divided cells during day 3 and 4 of *Xenia* regeneration. After EdU washout, shRNA was added on day 6 followed by FACS based quantification of EdU positive (+) and alga- containing cells. **d**, Quantification of the number of newly formed (EdU+) alga-containing endosymbiotic cells upon LePin RNAi. Each animal is normalized against the mean of the control shRNA within the same batch of experiment. Four batches of independent experiments were performed. Each dot stands for an animal. A total of 10-13 regenerating polyps were used for each shRNA treatment. **e**, The GEPs identified by NMF analysis. The cells are ordered along the trajectory of lineage progression. The relative expression of GEPs in each cell is indicated by the heatmap. **f-h**, The expression of GEPs 1 (f), 4 (g), 22 (h) in each cell along the lineage trajectory. Each dot stands for a cell in control or LePin shRNA treated samples. The box plot indicates the GEP expression (see Method) distribution for the cells within one pseudotime unit. Lines in the box represent the median; the upper and lower edges of the box represent the upper and lower quartiles, respectively. **i**, Knocking down Omph/FibL and Heme-binding2 in GEP 1 leads to the reduction of the newly formed alga-containing cells. Quantification as in (d). Each dot stands for an animal. 7-9 animals were used for each treatment. The p values of the unpaired Student's t-test are indicated in **d** and **i**.

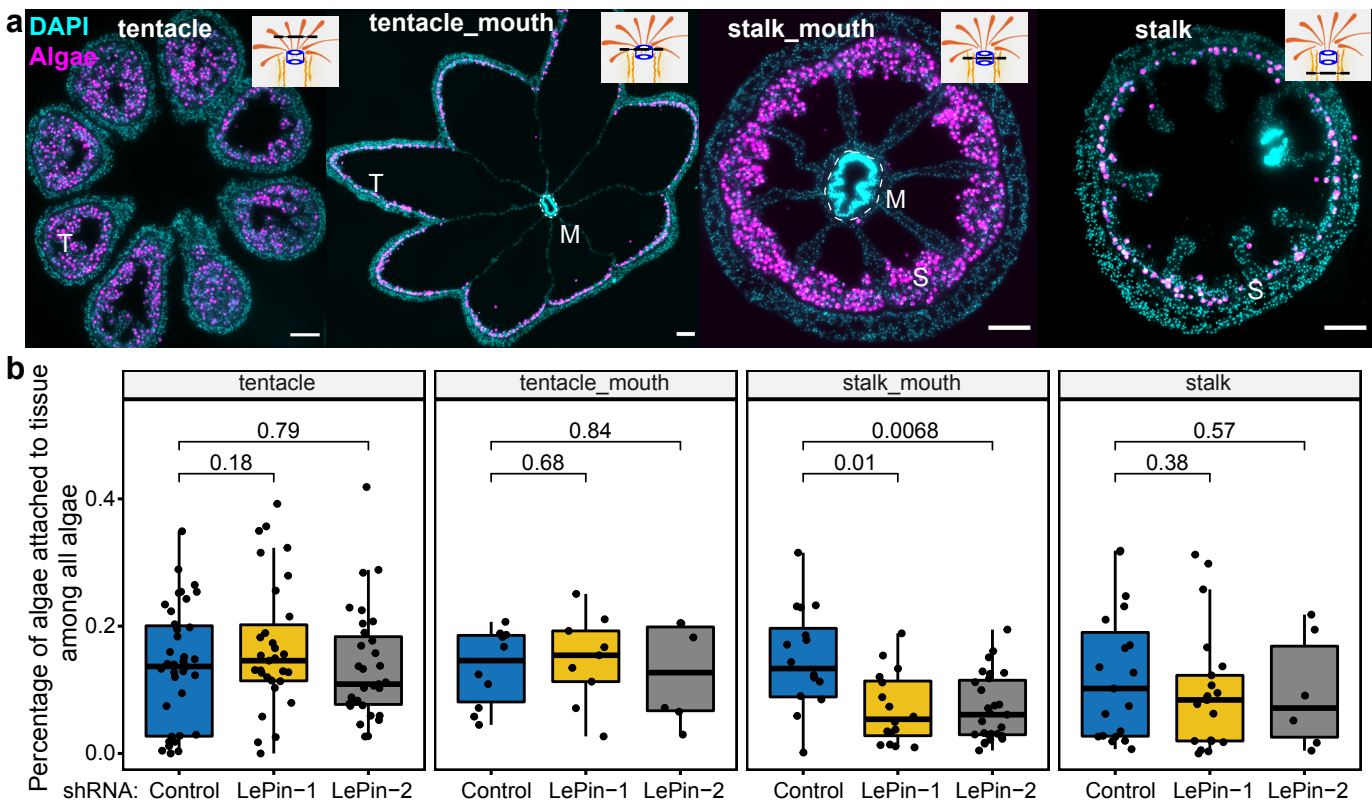


Fig. 3. LePin facilitates alga attachment to the stalk_mouth region of the gastrodermis. a, Single-plane epifluorescence images illustrating different tissue section categories. Algal cells were imaged by their autofluorescence and are displayed in magenta. Nuclei were stained with DAPI and are displayed in cyan. The black dashed lines in the polyp illustrations at the upper right corners of each panel indicate the positions of individual tissue sections. T, tentacle, M, mouth (outlined by white dotted circles), S, stalk. Scale bar, 100 μ m. **b**, Reduction of the number of algae attached to the tissues in the stalk_mouth region upon LePin RNAi. 12 regenerating polyps were used per shRNA treatment. Each dot stands for a tissue section. The p values of the unpaired Student's t-test are indicated.

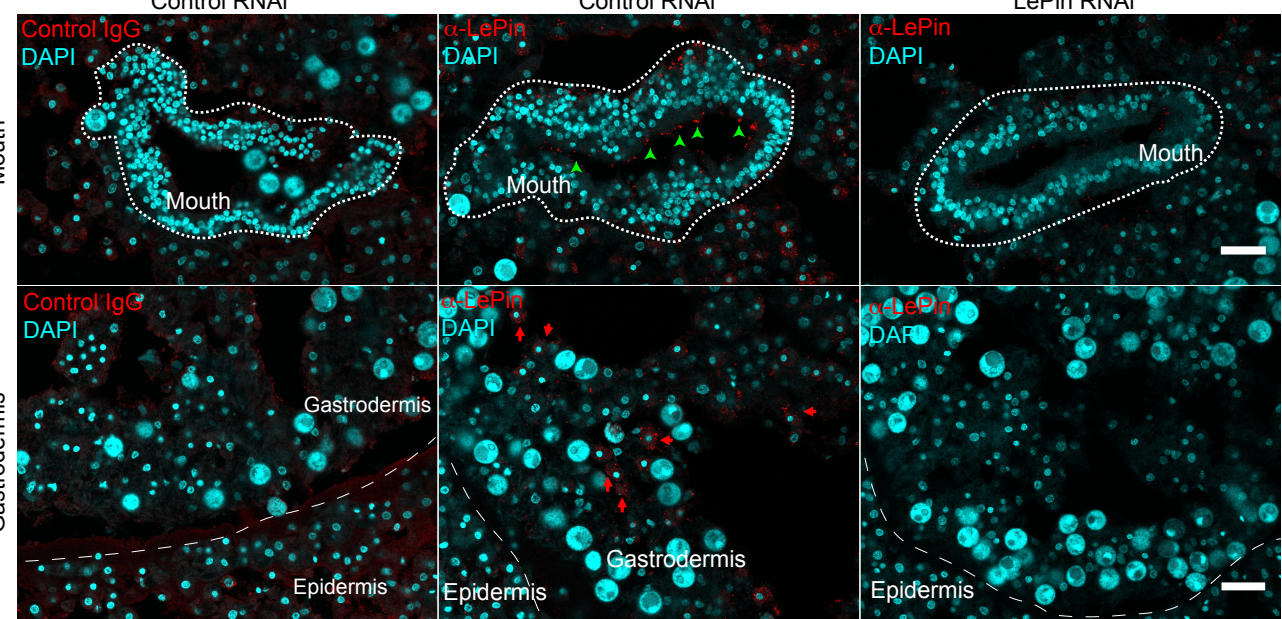
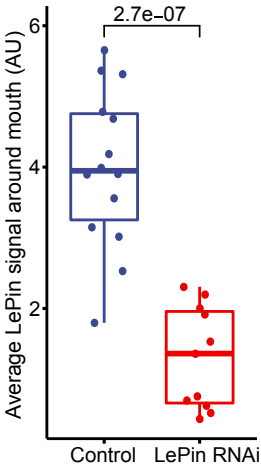
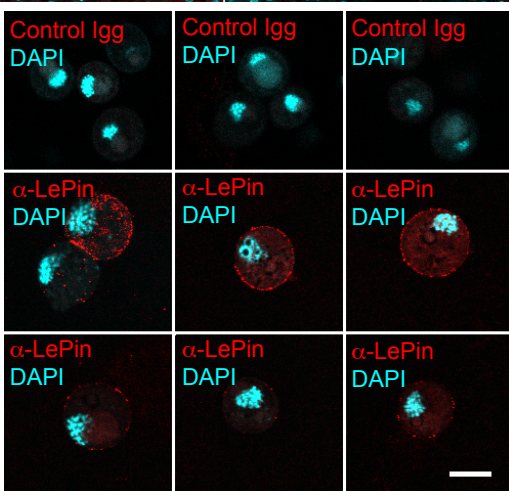
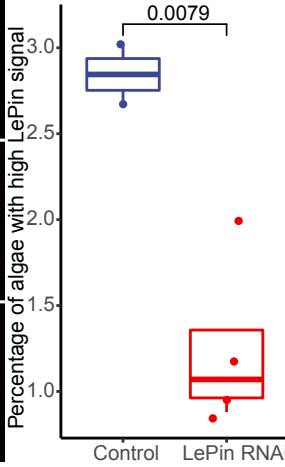
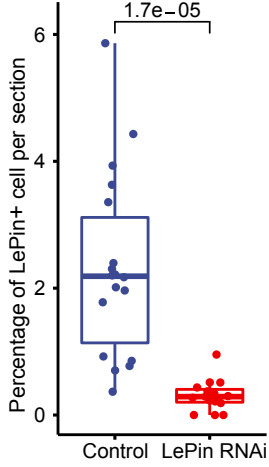
a**b****c****d****e**

Fig. 4. LePin in alga binding and recognition. a, Single-plane epifluorescence images illustrating control rabbit IgG or LePin antibody staining in the mouth (top) and gastrodermis (bottom) within the stalk_mouth region. Nuclei are stained with DAPI and displayed in cyan, while the LePin immunofluorescence signal is displayed in red. Green arrows indicate LePin signals around the mouth tissue. Red arrows indicate LePin signal in alga-free cells. Scale bar, 20 μ m. **b**, Quantification of LePin fluorescence signal intensity around the mouth structure. **c**, Control or LePin antibody staining of the free algae isolated from *Xenia*. LePin showed a range of immunostaining intensity. Scale bar, 10 μ m. **d**, Quantification of the percentage of isolated algae with high LePin signal by FACS (see Extended data Fig. 7 for detailed FACS gating and quantification). Each dot stands for a polyp. **e**, Quantification of the percentage of LePin positive and alga negative cells in all the cells in the tissue sections of the stalk_mouth region. The p values of the unpaired Student's t-test are indicated in **b**, **d**, **e**.

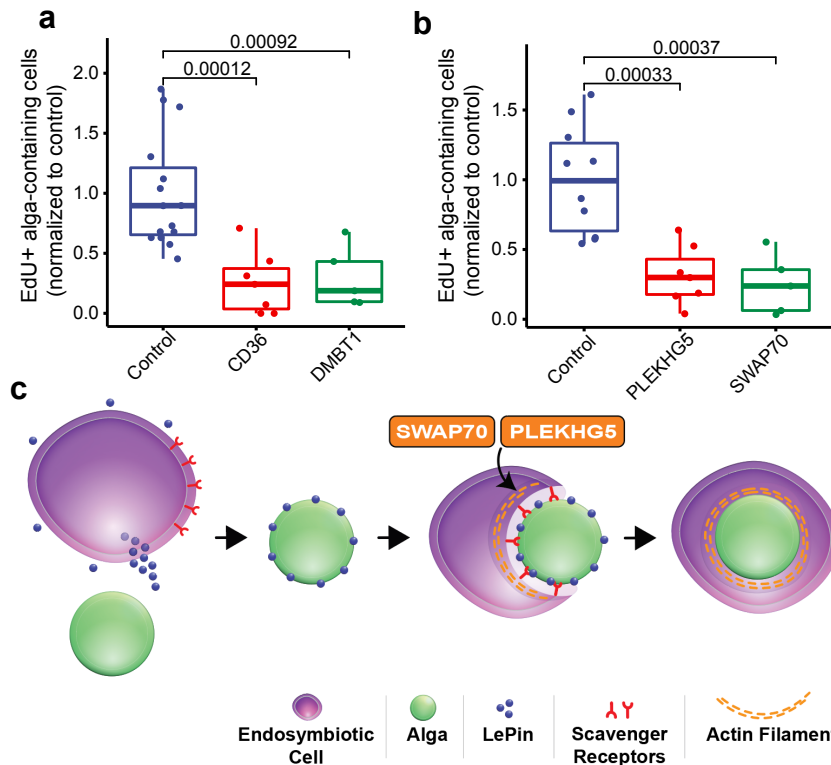
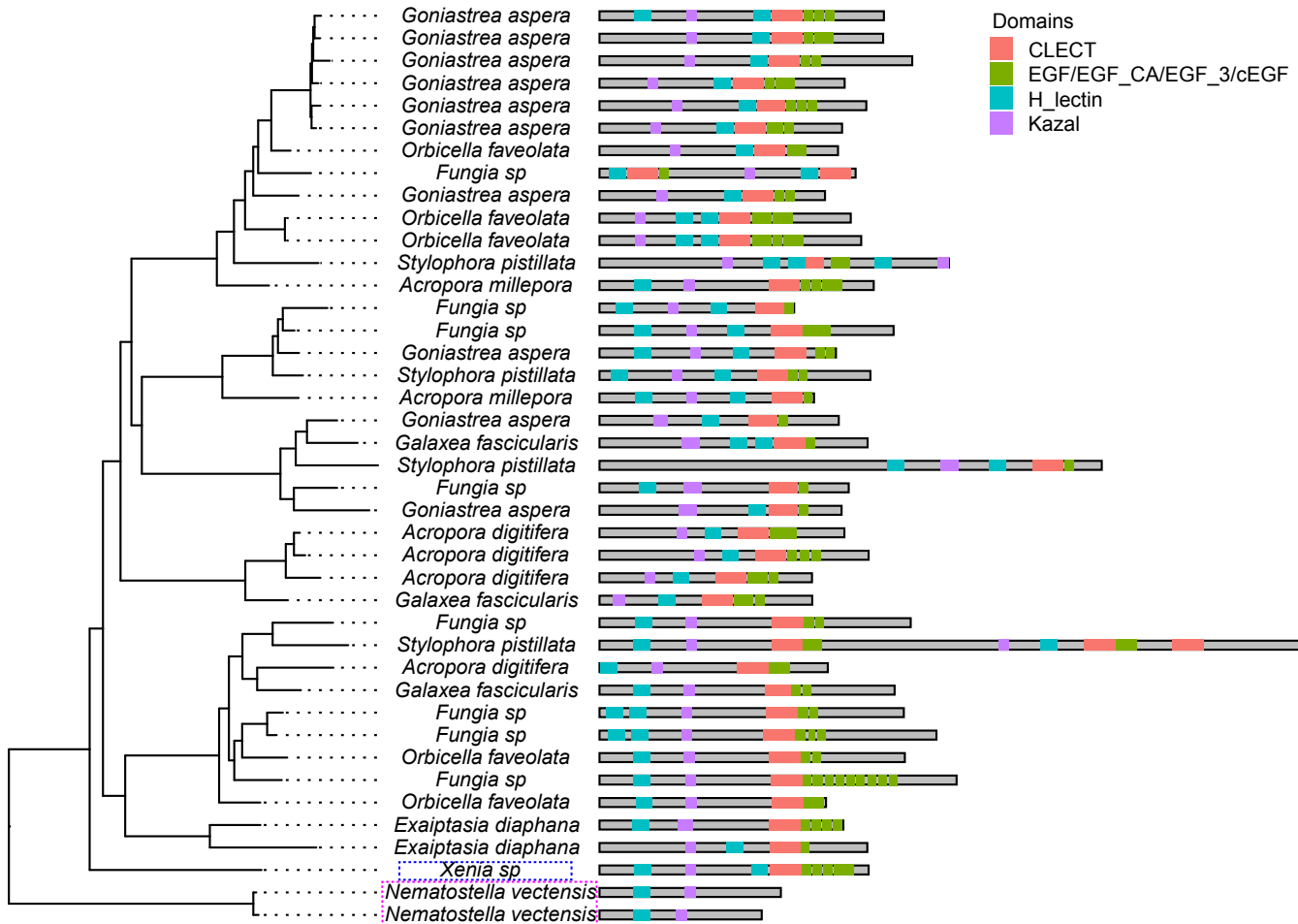
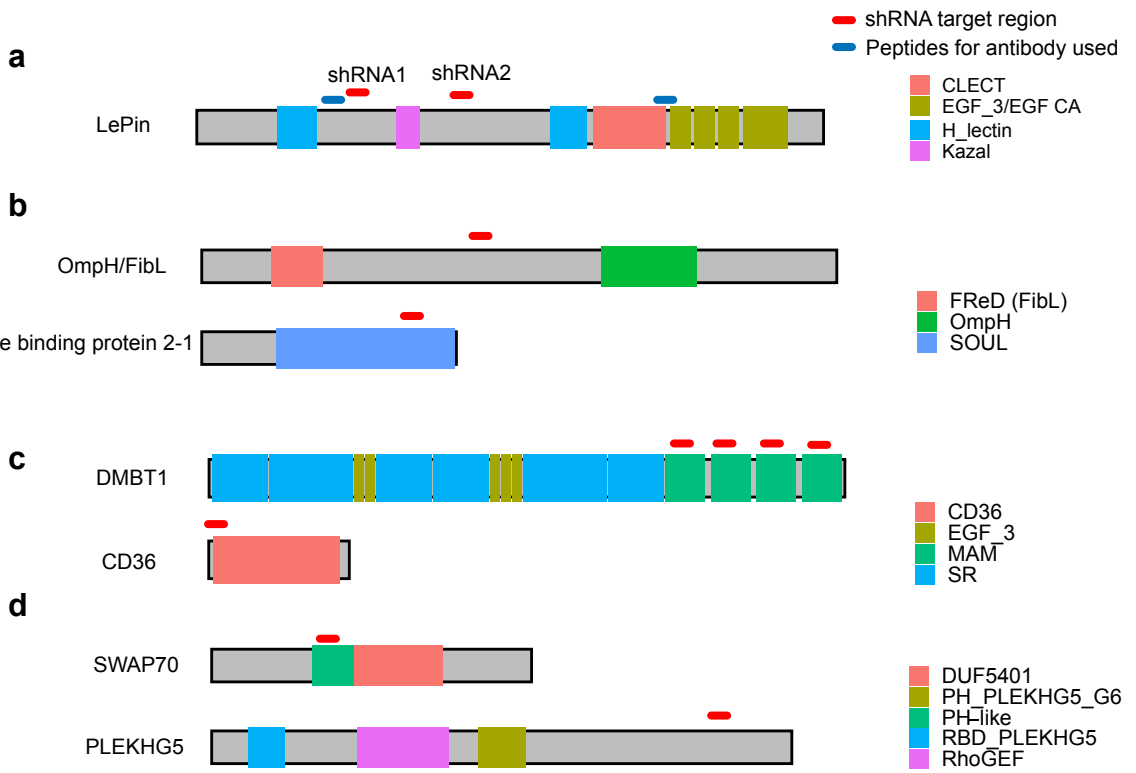


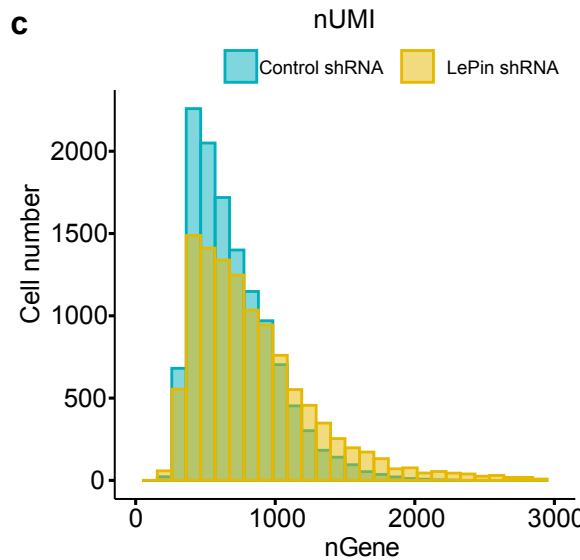
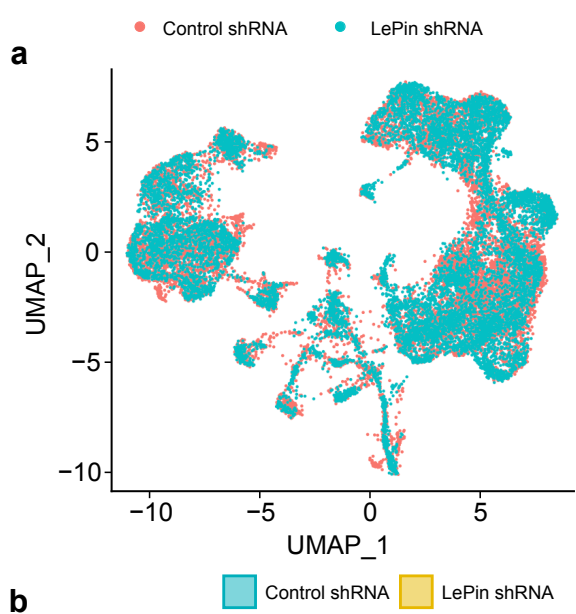
Fig. 5. scavenger receptors and actin regulators for endosymbiosis. a, b, shRNAs targeting scavenger receptors, CD36 and DMBT1 (a), or actin regulators, PLEKHG5 and SWAP70 (b), reduced the number of newly formed alga-containing endosymbiotic cells. Quantification is the same as in Fig. 2d. Each dot stands for a polyp. 5-9 polyps were used for each shRNA treatment. The p values of the unpaired Student's t-test are indicated. **c**, A model: the secreted LePin expressed in the endosymbiotic cells binds to alga and initiates alga recognition. This leads to the engagement of the scavenger receptors CD36 and DMBT1 and alga phagocytosis mediated by the actin regulators PLEKHG5 and SWAP70.



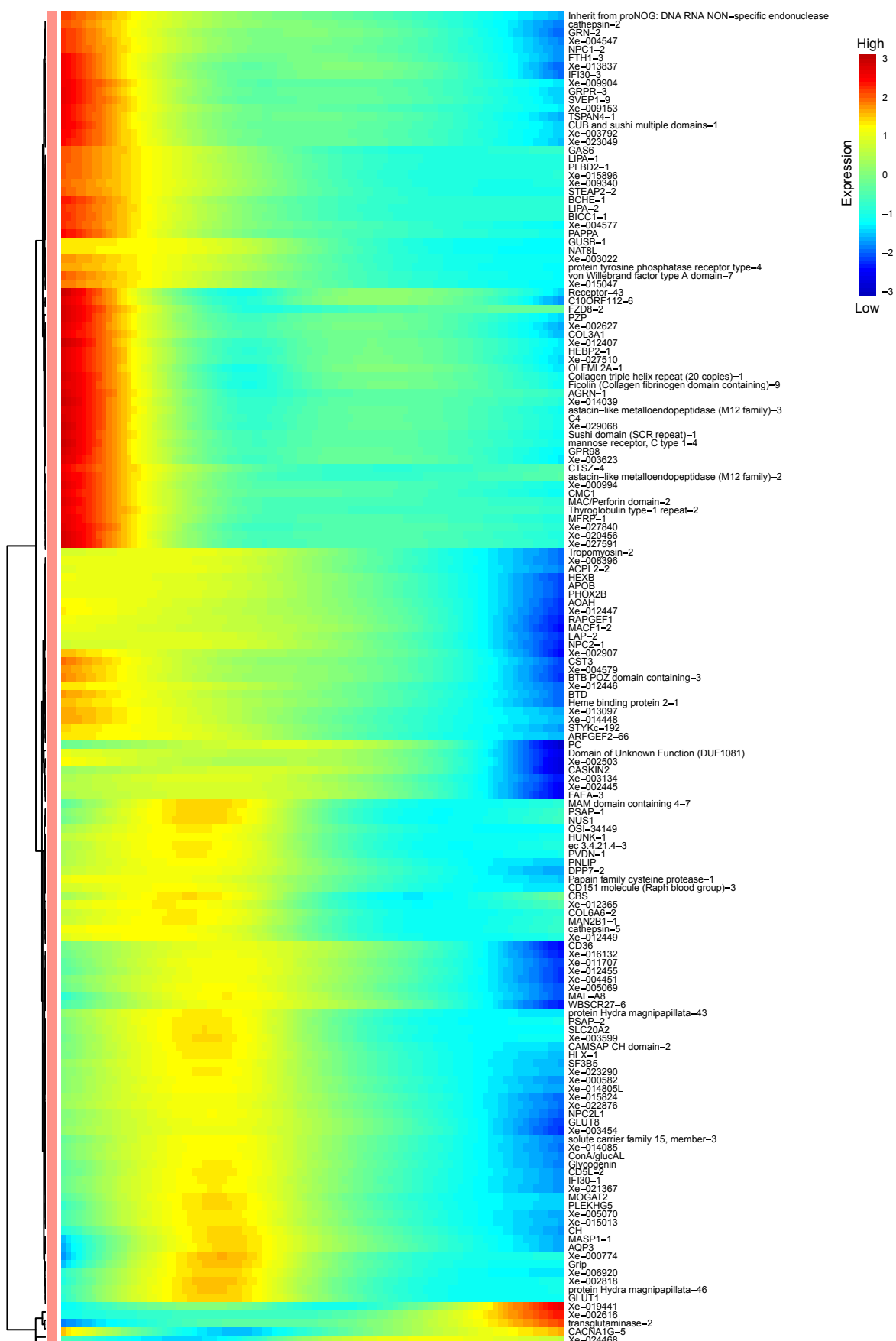
Extended Data Fig. 1. Domain organization of the predicted LePin-like proteins from different marine cnidarians plotted with the phylogenetic tree based on LePin sequences. CLECT: C type Lectin domain; EGF/EGF_Ca/EGF_3/cEGF: EGF, EGF-Calcium binding and EGF like domains (EGF_3 or cEGF); H_lectin: H type lectin domain; Kazal: kazal domain. *Xenia* LePin is highlighted by a dashed blue rectangle. The two lectins in *Nematostella vectensis* (highlighted by a dashed magenta rectangle) that are most similar to *Xenia* LePin miss a few domains and appear as an outgroup.



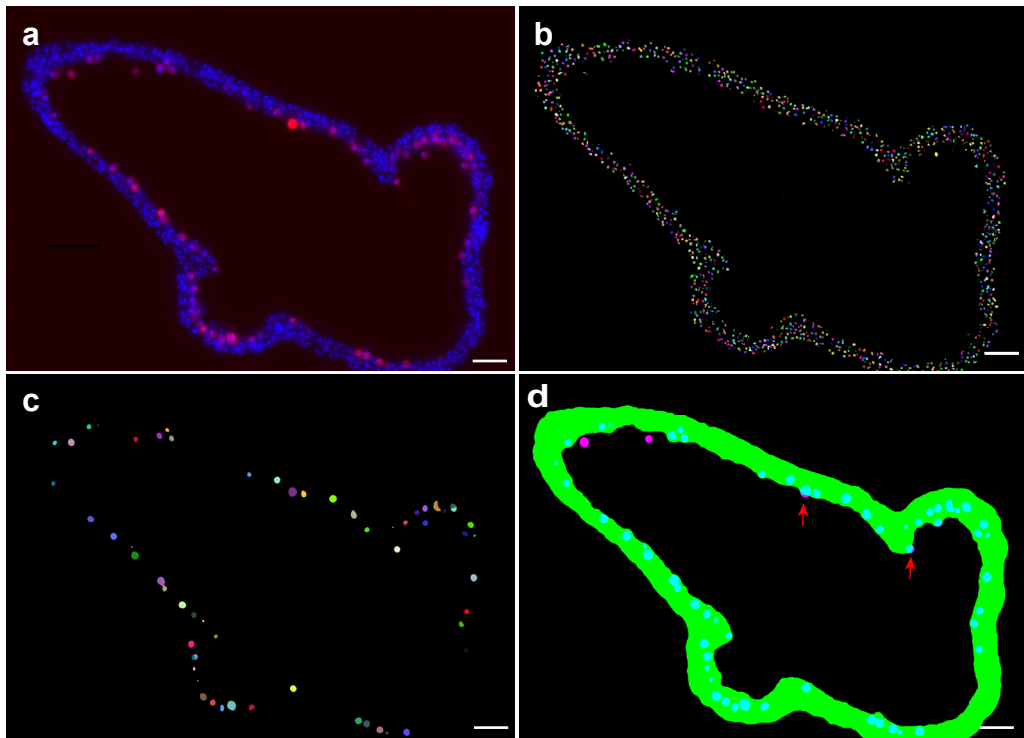
Extended Data Fig. 2. Illustration for proteins studied. Illustrations of domains and target regions of shRNA and peptides (for antibodies) for the proteins studied in this report.



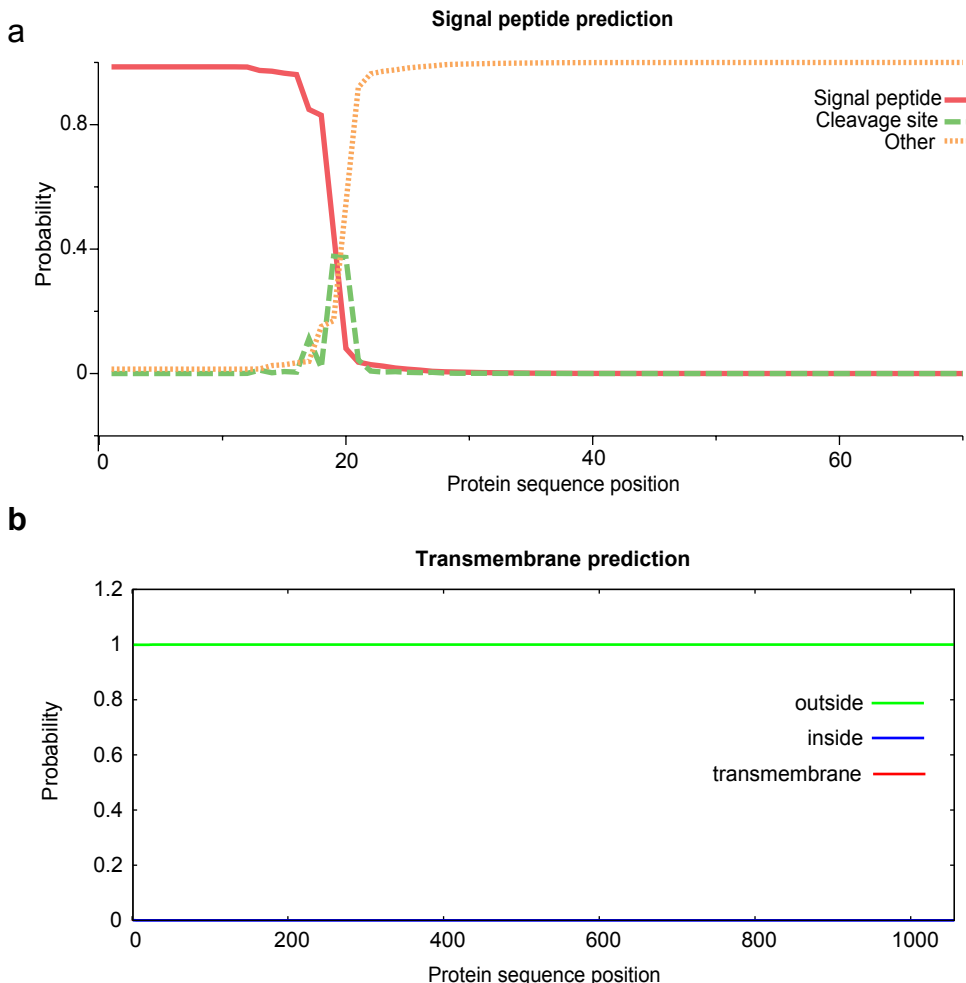
Extended Data Fig. 3. Additional analyses of scRNA-seq for RNAi-treated samples. a, The integrated UMAP of all cells from the control and LePin RNAi samples. **b, c,** Distributions of the detected UMI (Unique Molecular Identifier) numbers (**b**) and gene numbers (**c**).



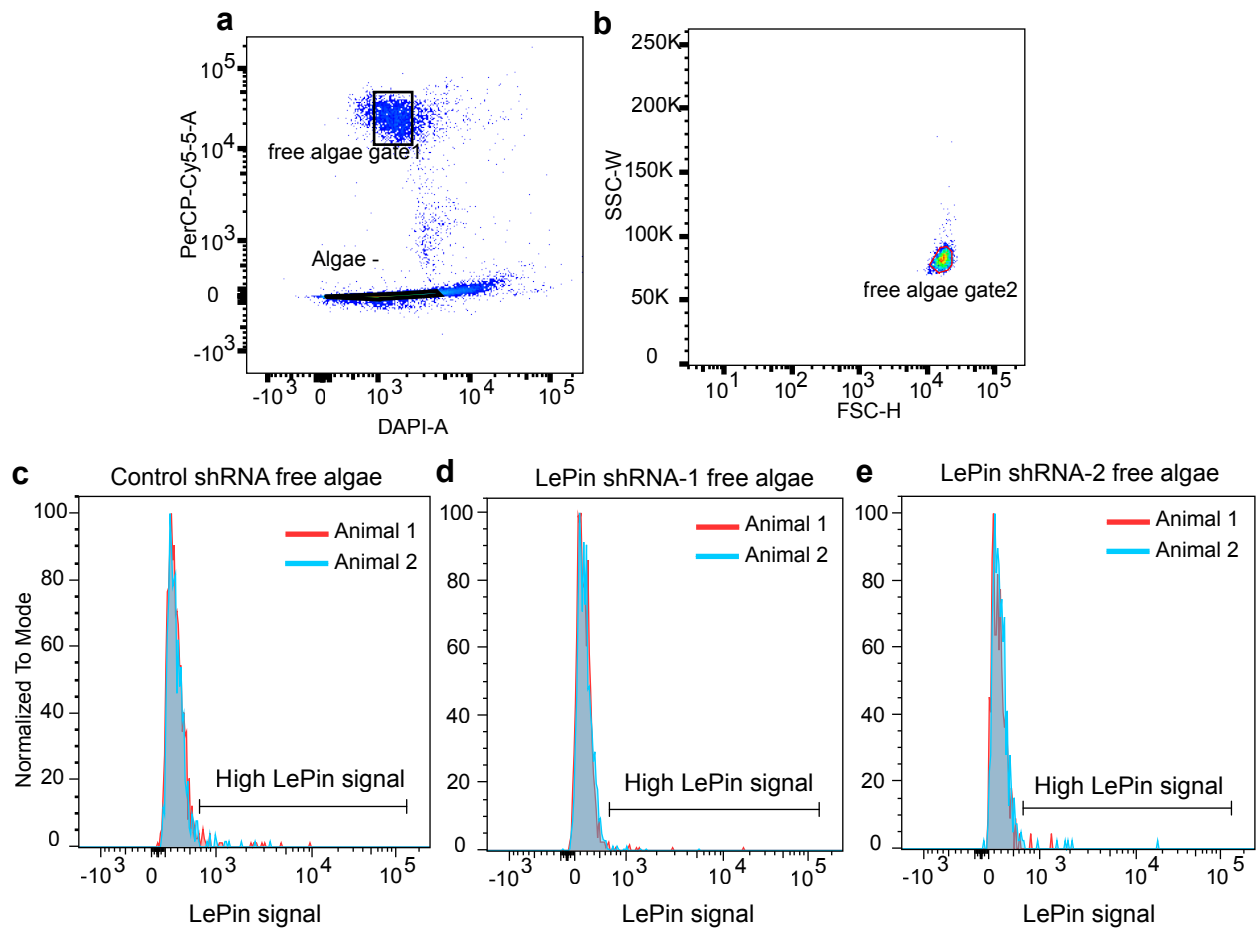
Extended Data Fig. 4. An expanded view of Fig. 2b to show the names of individual genes.



Extended Data Fig. 5. Unbiased high throughput quantification of algae attached to the surface of *Xenia gastrodermis*. **a**, An example of an epifluorescence image from a tissue section. Blue, DAPI staining of nuclei. Red, auto-fluorescence from the alga. **b**, Labeling of all cells by the DAPI signal. Each nucleus was pseudo colored to enable counting (see the Method section). **c**, Labeling of alga cells by the auto-fluorescence signal. Each alga was pseudo colored to enable counting (see the Method section). **d**, Tissue mask (green) is generated with a lower threshold of the DAPI signal and overlaid with the algal autofluorescence channel. The algae within the tissue mask are labeled blue. The algae outside or not completely inside the tissue mask are labeled pink. Red arrows point to the algae protruding from the tissue surface and are counted as algae attached to the surface of the gastrodermis. Scale bar, 50 μ m



Extended Data Fig. 6. Prediction of signal peptide and transmembrane sequences in LePin. **a**, the signal peptide is predicted by SignalP 5.0 with the Eukarya model. OTHER: no signal peptide predicted. Only the first 70 amino acids of LePin are plotted. **b**, LePin is predicted as a protein without transmembrane domain. TMHMM (v2.0) was used for the prediction. The full length LePin sequence is plotted.



Extended Data Fig. 7. Quantification of LePin signal on the isolated free algae in *Xenia* by FACS. **a,b**, Gating strategy for the free algae in *Xenia*. The algae are first gated based on the DAPI staining of the nuclei and algae autofluoresce (Cy5.5 signal) (**a**, free algae gate1). The algae are further gated based on the forward scatter (FSC) and side scatter (SSC) signals to further exclude those algae that are inside the *Xenia* cells (**b**, free algae gate2). **c-e**, LePin signal distribution on free algae in control (**c**) and LePin knocking down samples (**d,e**). Color codes for individual animals. The percentage of algae with high LePin signals (as indicated by the brackets) are quantified.

1 **Methods**

2 ***Xenia* culture and regeneration**

3 The *Xenia* colonies are grown in our aquarium as previously described⁴⁵. To
4 culture polyps in tissue culture plates, one or several colonies of *Xenia* is collected from
5 the aquarium and incubated in the Ca-free seawater (393.1 mM NaCl, 10.2 mM KCl,
6 15.7 mM MgSO₄·7H₂O, 51.4 mM MgCl₂·6H₂O, 21.1 mM Na₂SO₄, and 3 mM NaHCO₃,
7 pH 8.5) for 15 min to relax the animals. Individual polyps are cut from the colony and
8 transferred into a well of 24 well plates with 2 ml of seawater. Colony health is important
9 for good regeneration. High polyp lethality rates after transplanting to tissue culture
10 plates generally lead to poor regeneration. We only perform the follow up experiments
11 and analyses if the survival rate is >80%. The plates are incubated at 25°C in a Percival
12 incubator with a cycle of 12 hours light on and 12 hours of light off. The polyps are
13 allowed to recover for a week after transplantation before performing the follow up
14 experiments. For *Xenia* regeneration, all 8 tentacles are surgically cut away and the
15 stalk attached to the plate is allowed to regenerate by further incubation.

16

17 **shRNA design and production**

18 The shRNA target sequences are designed using the Invitrogen's siRNA Wizard
19 site (<https://www.invivogen.com/sirnawizard/design.php>) with 19 nucleotides as the
20 motif length, targeting a given gene. The 19 nucleotide sequences selected have 40-
21 50% GC content and no more than four consecutive thymidines (T). These selected
22 candidate sequences are then blasted against the *Xenia* transcriptome to select the
23 ones with specific hits to the target gene. The T3 promoter sequence (5'

24 AATTAACCCTCACTAAAG 3') is added to the 5' of these targeting sequences followed
25 by adding the loop sequence (5'-TTCAAGAGA-3') to the 3' end of the target sequence
26 and then the reverse complementary sequence of the target sequence. Two additional
27 Ts are then added to the 3' end of the synthetic sequence, which gives rise to the
28 shRNA primer1. Both shRNA primer1 and its reverse complementary strand (shRNA
29 primer2) are synthesized as DNA oligos. To confirm the stem loop structures, we used
30 the mfold Web Server (<http://unafold.rna.albany.edu/?q=mfold/RNA-Folding-Form>) to
31 evaluate stem-loop structures. The two complementary DNA oligos are mixed in equal
32 molar (0.2 pM each for 20 μ l reaction) and used as the template for *in vitro* transcription
33 by MEGAscriptTM T3 Transcription Kit (Invitrogen, AM1338). After transcription, 1 μ l
34 DNase I (AmbionTM) is added for each 20 μ l reaction. The DNA templates are removed
35 by incubating at 37 °C for 30 min. To purify the shRNA, one-tenth volume of 3 M NaOAc
36 (pH 5.5), and 3 volumes of ice-cold 95% ethanol are added into the reaction. shRNA is
37 precipitated at -80°C for 30 min, followed by centrifuging at 14,000 rpm for 15 min at
38 4°C. The pellet is washed twice with 500 μ l ice-cold 80% ethanol and air dried at room
39 temperature. The shRNA is further dissolved in DEPC-treated water and the
40 concentration is determined by Nanodrop. The sequence information for all the shRNA
41 oligos used in this study is listed in Supplementary table 1 and the target positions of
42 these oligos in the corresponding proteins are indicated in Fig. S2.

43

44 **shRNA treatment of *Xenia* polyps**

45 Each intact polyp or regenerating polyp is cultured in a well of 24 well plates.
46 After tentacle amputation, healthy polyps under good culturing conditions grow a clear

47 set of short tentacles by day 3 and the tentacles continue to extend in subsequent days.

48 The polyps with regeneration delays are excluded for RNAi experiment. For RNAi
49 treatment, the sea water in each well is replaced with 500 μ l fresh sea water containing
50 20 μ g shRNA. The animals are incubated for 3 hours followed by adding an additional
51 500 μ l fresh sea water. The animals are further incubated for 3 days before further
52 analyses. When healthy intact polyps or regenerating polyps are used, we have not
53 observed death caused by shRNA treatment.

54

55 **Edu pulse-chase and shRNA treatment of regenerating *Xenia* polyps to analyze
56 the newly formed alga-containing endosymbiotic cells**

57 The tentacle amputated *Xenia* polyps are allowed to regenerate and 1 mM EdU
58 is added to label the proliferating cells on day 3 and incubated for 48 hours. EdU is
59 washed away using sea water and the polyps are incubated further. The cells that
60 contain algae and are EdU positive are newly formed alga-containing endosymbiotic
61 cells. These cells are quantified by FACS as previously described¹. Our previous
62 studies have shown that the number of newly formed alga-containing endosymbiotic
63 cells continue to increase until the regeneration day 15⁴⁵. The regenerating polyps are
64 then treated with shRNA on day 6. FACS analysis is performed four days after shRNA
65 addition at the end of regeneration day 9.

66

67 **Single cell RNA sequencing (scRNA-seq)**

68 The scRNA-seq is carried out using the 10x Genomics platform as we previously
69 described¹. Briefly, two regenerating *Xenia* polyps treated by control RNAi or LePin

70 RNAi from regeneration day 6 to the end of regeneration day 9 (4 days) are digested
71 with 1 ml digestion buffer, containing 3.6 mg/ml dispase II (Sigma, D4693), 0.25 mg/ml
72 liberase (Sigma, 5401119001), 4% L-cysteine in Ca-free seawater. After one hour
73 incubation at room temperature, the polyps are dissociated into single cell suspension.
74 After tissue dissociation, fetal bovine serum is added to a final concentration of 8% to
75 stop enzymatic activities. The cell suspension is filtered through a 40- μ m cell strainer
76 (FALCON) twice. Approximately 17,000 cells per sample are used for single-cell library
77 preparation using the 10x Genomics platform with Chromium Next GEM Single Cell 3'
78 GEM, Library and Gel Bead Kit v.3.1 (PN-1000121, v.3 chemistry), Chromium Next
79 GEM Chip G Single Cell Kit (PN-1000127), and i7 Multiplex Kit (PN-120262) according
80 to manufacturer's manual. Libraries are sequenced using Illumina NextSeq 500 for
81 paired-end reads. In order to reduce batch effect, the control and LePin RNAi treated
82 samples are loaded in two wells in one 8-well strip and sequenced at the same time.
83 Sample preparations are carried out simultaneously with multiple channel pipette.

84

85 **LePin antibody generation, purification, and antibody immunofluorescence**
86 **microscopy**

87 Three LePin peptides, KHNTSNNNVDPKYNA, NKNHPTSENNYAYCK,
88 KNYTCQKDYDECGEN, are selected based on the high antigenicity and surface
89 probability of the LePin protein sequence. A cysteine is added to the N terminus of each
90 peptide for coupling chemistry and the peptides are synthesized by GenScript (Inc.).
91 The purity of the three peptides are 96.9%, 90.5% and 85.3%, respectively. The
92 antibodies are produced at Pocono Rabbit Farm & Laboratory (Inc.) using the 28 day

93 mighty quick protocol. The second and third peptides are combined and injected into
94 two rabbits (#36232, #36243), while two additional rabbits (#36230,#36231) are
95 immunized by the first peptide. To assess the sera, each is used for immunostaining of
96 *Xenia* tissue sections. The sera from three rabbits (#36231, #36232, #36243) exhibit
97 stronger immunofluorescence signals than the corresponding control pre-immunization
98 sera.

99 The LePin antibodies from the serum of rabbit (#36232) is affinity purified using
100 the corresponding LePin peptides (NKNHPTSENNYAYCK and
101 KNYTCQKDYDECGEN). Briefly, the LePin peptides are coupled to an affinity column
102 with SulfoLink® Immobilization Kit (Thermo Scientific™, Cat. 44995) according to the
103 manufacturer's manual. The serum is slowly loaded onto the column twice over at least
104 2 hours. The column is washed with 10 column volumes of Tris-buffered saline (TBS, 20
105 mM Tris, 150 mM NaCl, PH7.4), followed by additional washing with 10 column volumes
106 of the washing buffer containing 0.5 M NaCl, 20 mM Tris HCl, pH 7.4, 0.2% Triton X-
107 100. After one more washing with 10 column volumes of washing buffer, the antibody is
108 eluted with 0.2 M glycine, pH 2.0. The eluate is collected at 3 ml/fraction into tubes
109 containing 0.2 ml 2 M Tris base (pH 11). The protein concentration of each fraction is
110 measured at OD280. The fractions with OD280>0.1 are pooled and dialyzed against 2L
111 TBS overnight at 4°C. The antibody solution is further concentrated by placing the
112 dialysis bags in Aquacide. Aliquots of 0.5 ml of the concentrated antibody are snap
113 frozen in liquid nitrogen and stored at –80°C. Upon usage, an aliquot is thawed at room
114 temperature and further concentrated with a 100 kDa Ultra-0.5 Centrifugal Filter Unit
115 (Amicon™) to a concentration of 2.2µg/µl.

116 The antibody staining is carried out according to the previous publication⁴⁶ with
117 minor modifications. Briefly, the polyps are pretreated with 2% ice-cold HCl for 3
118 minutes to remove mucus⁴⁷ and then fixed with 4% paraformaldehyde (PFA) for 15 min
119 at room temperature. After washing twice with PBST (0.5% triton X-100 in PBS: 137
120 mM NaCl, 2.7 mM KCl, 10 mM Na₂HPO₄, and 1.8 mM KH₂PO₄), the polyps are
121 transferred to 30% sucrose and incubated overnight at 4°C. Polyps are then embedded
122 in Tissue-Tek O.C.T. and subjected to cryosection at 12 µm thickness. The slides
123 containing tissue sections are rehydrated by incubating with PBST for 10 min for three
124 times. The slides are then blocked with 10% goat serum (Sigma, G9023) in PBST for 40
125 min at room temperature. The affinity purified LePin antibodies from rabbit #3264 or
126 rabbit IgG isotype control (invitrogen, Cat. 10500c) are diluted to 22 ng/µl with 10% goat
127 serum and used to incubate with the slides overnight at 4°C. After washing with PBST
128 three times 10 min each, the secondary antibody (Goat anti-Rabbit IgG, Invitrogen,
129 1:400 dilution,) and DAPI are applied to the slides. The slides are incubated at room
130 temperature for 1 hour, followed by washing with PBST three times, 10 min each. Slides
131 are mounted with ProLong™ Gold Antifade Mountant (Invitrogen™, P36930). The
132 images are acquired with a confocal microscope (Leica).

133

134 **LePin phylogenetic analyses**

135 To build LePin phylogenetic tree among marine anthozoans with available
136 sequence information, Blastp(v2.1.2) is used to find the potential *LePin*-like genes with
137 parameter -max_target_seqs 5000 -max_hsps -evalue 1e-10. The homologous
138 regions in a given protein sequence that cover less than 60% of the *Xenia* LePin are

139 filtered out. For the marine anthozoans known to do endosymbiosis with algae, the
140 genes without the predicted KAZAL, EGF, CLECT, H_lectin domains are also excluded.
141 The phylogenetic tree is built by ETE toolkit (v.3) with the standard_trimmed_fasttree
142 workflow⁴⁸. Domain information for each gene is fetched from NCBI CDD domain
143 database (April 02, 2019 version)⁴⁹.

144

145 **NMF analyses of the scRNA-seq datasets**

146 scRNA-seq analysis is carried out as previously described with minor
147 modifications⁴⁵. Briefly, the gene expression matrix for each cell is generated by
148 cellranger(v3.1). Cells with mitochondrial gene expression higher than 0.2% of all reads
149 or UMI values lower than 400 were excluded. Potential doublets as identified by
150 DoubletFinder (v2.0.3)⁵⁰ are excluded before subsequent analysis. The endosymbiotic
151 cells from LePin and control RNAi samples are identified by Seura(v3.0.2)⁵¹ label
152 transfer method using our previous *Xenia* scRNA-seq data⁴⁵ as reference and subject to
153 monocle2 (v2.12.0)⁵² for lineage trajectory prediction.

154 The NMF analysis is carried out according to the previous publication⁵³. Briefly,
155 we applied the NMF analysis on the scRNA-seq data for the endosymbiotic cell lineage.
156 To select the highly variable expression genes, the 3000 variable genes from control or
157 LePin RNAi are identified with Seurat FindVariableFeatures functions. These genes are
158 combined together which leads to a total of 5194 variable genes. The NMF analysis is
159 based on previously published NMF framework (<https://github.com/YiqunW/NMF>) and
160 performed with log-normalized expression of the variable genes in all endosymbiotic
161 cells using the run_nmf.py function with the default parameters. K=45 is selected and

162 the Gene Expression Programs (GEP) with low reproducibility between different runs
163 excluded as previously described⁵³. The NMF analysis will generate two matrices. One
164 is GEP-gene matrix, which shows the relative contribution of each gene (also called
165 gene weight) to the GEP. The other is the GEP-cell matrix, which shows the relative
166 expression of GEP (also called GEP weight) to each cell. The GEPs that only contain
167 genes with low weight (<0.6) are also excluded from further analysis of the effect of
168 LePin in GEP expression along the endosymbiotic lineage development. The relative
169 expression of each GEP is used to indicate the GEP activity for each cell and plotted
170 along the pseudotime trajectory (Supplementary Table S3). Cells are grouped into
171 control or LePin RNAi samples to further explore the GEP activity change upon LePin
172 RNAi.

173

174 **Data availability**

175 We have uploaded all raw data to NCBI (PRJNA869069). The *Xenia* genome is
176 also available at NCBI (Genebank accession: JAJSR000000000.1). Select
177 intermediate RDS objects are available at figshare
178 (https://figshare.com/articles/dataset/Processed_R_objects_for_LePin_RNAi_/20481900).
179

180

181 **Code availability**

182 All analysis codes for scRNA-seq and alga counting are available at GitHub:
183 https://github.com/MinjieHu/Xenia_RNAi.

184

185 **References**

186 45. Hu, M., Zheng, X., Fan, C.-M. & Zheng, Y. Lineage dynamics of the endosymbiotic cell
187 type in the soft coral *Xenia*. *Nature* **582**, 534–538 (2020).

188 46. Hu, M. *et al.* Liver-Enriched Gene 1, a Glycosylated Secretory Protein, Binds to FGFR and
189 Mediates an Anti-stress Pathway to Protect Liver Development in Zebrafish. *PLOS Genet.* **12**,
190 e1005881 (2016).

191 47. Forsthoefel, D. J., Ross, K. G., Newmark, P. A. & Zayas, R. M. Fixation, processing, and
192 immunofluorescent labeling of whole mount planarians. *Methods Mol. Biol. Clifton NJ* **1774**,
193 353–366 (2018).

194 48. Huerta-Cepas, J., Serra, F. & Bork, P. ETE 3: Reconstruction, Analysis, and Visualization of
195 Phylogenomic Data. *Mol. Biol. Evol.* **33**, 1635–1638 (2016).

196 49. Lu, S. *et al.* CDD/SPARCLE: the conserved domain database in 2020. *Nucleic Acids Res.*
197 **48**, D265–D268 (2020).

198 50. McGinnis, C. S., Murrow, L. M. & Gartner, Z. J. DoubletFinder: Doublet Detection in
199 Single-Cell RNA Sequencing Data Using Artificial Nearest Neighbors. *Cell Syst.* **8**, 329-337.e4
200 (2019).

201 51. Stuart, T. *et al.* Comprehensive Integration of Single-Cell Data. *Cell* **177**, 1888-1902.e21
202 (2019).

203 52. Trapnell, C. *et al.* The dynamics and regulators of cell fate decisions are revealed by
204 pseudotemporal ordering of single cells. *Nat. Biotechnol.* **32**, 381–386 (2014).

205 53. Siebert, S. *et al.* Stem cell differentiation trajectories in Hydra resolved at single-cell
206 resolution. *Science* **365**, eaav9314 (2019).

207 **Acknowledgements**

208 We thank Fred Tan and Alison Pinder for assistance with all the sequencing and initial
209 processing of raw reads; Navid Marvi for the model sketch; and Lynne Hugendubler and
210 Mike Watts for maintaining the coral aquarium; Ross Pedersen and Joseph Tran for
211 critical comments. This work is supported by Gordon and Betty Moore Foundation,
212 Aquatic Symbiosis no. GBMF9198 (<https://doi.org/10.37807/GBMF9198>, Y.Z.).

213

214 **Author information**

215 Authors and Affiliations

216 Department of Embryology, Carnegie Institution for Science, Baltimore, MD, USA

217 Minjie Hu, Yun Bai, Xiaobin Zheng & Yixian Zheng

218

219 **Contributions**

220 M.H. and Y.Z. conceived the project. M.H. and Y.Z. designed experiments. M.H. and

221 Y.B. performed the experiments. M.H. and X.Z. analysed the data. M.H., Y.B., X.Z. and

222 Y.Z. interpreted the data. M.H. and Y.Z. wrote the manuscript.

223

224 **Corresponding authors**

225 Correspondence to Minjie Hu or Yixian Zheng.

226

227 **Ethics declarations**

228 Competing interests

229 The authors declare no competing interests.

230

231 **Additional information**

232 Supplementary Information is available for this paper.

233

234 **Supplementary Table S1. The list of genes/proteins studied.** The shRNA and
235 predicted protein sequences are listed along with the gene names. We manually
236 checked each gene to confirm that it has reads mapping to all their exons using
237 transcriptomic data.

238

239 **Supplementary Table S2. The top 30 genes for each of the 24 GEPs.** The first sheet
240 contains the list of 30 genes in each GEP. Each GEP has two columns. The first column
241 shows the top 30 genes. The second column indicates the weight of each gene. The
242 second sheet (related gene id and sequence) shows the protein sequence and the gene
243 ID of the genes shown in the first sheet.

244

245 **Supplementary Table S3. Expression of each GEP along the pseudotime for each**
246 **endosymbiotic cell.** The cell identity comes from the cell barcode together with sample
247 information. The pseudotime value for each cell is calculated by the lineage trajectory
248 analysis with Monocle2. The relative expression of each GEPs is calculated by NMF
249 analysis.